



# Numerical analysis of excimer laser-induced breakdown of Kr gas

Kholoud A. Hamam<sup>1</sup> · Khaled A. Elsayed<sup>2,3</sup> · Yosr E. E. Gamal<sup>4</sup>

Received: 18 November 2016 / Accepted: 20 January 2017 / Published online: 10 March 2017  
© Springer-Verlag Berlin Heidelberg 2017

**Abstract** The present paper displays a numerical study on the role of electron dynamics in relation to the dependence of the threshold intensity on the pressure in the breakdown of gases by laser radiation. The analysis aimed to find out the origin of the steep slope observed in the measurements of threshold intensity against gas pressure in the breakdown of Kr induced by an excimer laser source (Opt. Commun. 13:66–68, 1997). The experiment was carried out using wavelength 248 nm and pulse width of 18 ns for a gas pressure range 4.5–300 torr. The investigation centered on an adaptation of our previously developed electron cascade model given in Evans and Gamal (J. Phys. D Appl. Phys. 13:1447–1458, 1980). This model solves numerically a time-dependent energy equation simultaneously with a set of rate equations that describe the change of the population of the formed excited states. The modifications introduced into the model the realistic structure of the krypton gas atom as well as electron diffusion as a loss process to inspect the experimentally tested low-pressure regime. A computer program is undertaken to determine the breakdown threshold intensity as a function of gas pressure. Reasonable agreement is obtained between the calculated thresholds and measured ones, corresponding

to the examined pressure range. This agreement validates the applicability of the model. The relationship between the role of the physical mechanisms and gas pressure is studied by analyzing the EEDF and its parameters at selected pressure values that cover the experimentally tested range. The result of this study clarified that electron diffusion out of the focal region is responsible for the steep slope of the threshold intensities for pressures <75 torr. For higher pressures (75–300 torr), collisional excitation of ground-state atoms followed by their ionization via multiphoton and collisional processes acts to convert the Kr gas in the interaction region into the state of breakdown. Investigation of the temporal of the EEDF for the selected pressure values showed non-Maxwellian distribution as well as determined the time and energy region at which breakdown is formed.

## 1 Introduction

In this work, a numerical model is applied to find out the origin of the unexpected steep slope observed experimentally in the measurement of the dependency of the breakdown threshold intensity on the Kr gas pressure over pressure range 4.5–300 torr [1]. The breakdown was created by an excimer laser source of wavelength 248 nm and pulse width of 18 ns. No explanation was given for this observation. The analysis is grounded on a modification of the electron cascade model that earlier developed by Evans and Gamal [2] and applied in Refs [3–7]. The modified model considered more realistically the structure of the krypton atom as well as the most physical mechanisms that might occur corresponding to the applied experimental conditions. The main feature of the model is to solve numerically a time-dependent equation for the distribution of electrons energy, besides the rate equations, which describe the

✉ Khaled A. Elsayed  
kelsayed@niles.edu.eg

<sup>1</sup> Department of Physics, Girl's Faculty of Science, King Abdul-Aziz University, Jeddah, Kingdom of Saudi Arabia

<sup>2</sup> Department of Physics, Faculty of Science, Cairo University, Giza, Egypt

<sup>3</sup> Department of Basic Sciences, College of Engineering, University of Dammam, Dammam, Kingdom of Saudi Arabia

<sup>4</sup> National Institute of Laser Enhanced Sciences, Cairo University, Giza, Egypt

variation of the population of the produced excited atoms. This energy equation includes processes acting as sources for seed electrons (multiphoton ionization, and inverse Bremsstrahlung) as well as mechanisms responsible for the fast accumulation of electrons concentration (cascade ionization by collision). Experimentally, it has been shown that krypton gas atoms suffer from a Ramsauer minimum, in the variation of the momentum transfer collision cross section with the electron energy [13]. This decrease could have an obvious effect on the rate of energy gained by electrons from the laser field during the inverse Bremsstrahlung absorption process. This process has a pronounced role in the breakdown of krypton. The modification of the model treated the Kr atom is as a four-state atom namely: a ground state, an ionized state, and two excited states. Also, the model introduced electrons diffusion out of the interaction region as an electron loss process. For more reasonable results, the analysis accounted for the dependence of the rate coefficients and cross sections of the involved physical mechanisms on the electron energy. A computer program is undertaken to calculate; firstly, the threshold intensity as a function of gas pressure for model validation; secondly, to analyze the EEDF and its parameters at selected values of the gas pressure. This analysis aimed to explore the physical processes which controlling the breakdown phenomenon over the experimentally tested pressure range.

## 2 Modeling background

### 2.1 Formulation

A full study of the applied theoretical treatment used to explain the electron collision model is specified in our earlier paper [2]. Here we review only the outlines of this model. Following the adopted structure of the Kr atom, the model considers the subsequent collisional and radiative processes as gain and loss mechanisms for electrons and their energy. (1) Absorption of energy by electrons through the inverse-Bremsstrahlung process; (2) excitation by electron impact of atoms in the lower state by electrons of energy  $\varepsilon > 9.91$  eV; (3) excitation by electron impact of atoms in the upper state by electrons of energy  $\varepsilon > 10.03$  eV; (4) collisional ionization of ground-state atoms by electrons having energies  $\varepsilon > 14.0$  eV; (5) collisional ionization of the lower excited state atoms by electrons possessing energy  $\varepsilon > (14.0-9.91)$  eV; (6) collisional ionization of the upper excited state atoms by electrons having the energy  $\varepsilon > (14.0-10.03)$  eV; (7) photo-ionization of the atoms in the lower excited state; (8) photoionization of atoms in the upper excited state, and (9) electron diffusion losses.

For krypton atoms corresponding to the tested experimental conditions [1] we neglected both superelastic collisions from the electronically excited states and recombination losses.

Consequently, the time-dependent energy equation for distribution of the electron energy which represents variation of the energy gained by electrons from the laser field is given by:

$$\frac{\partial n(\varepsilon, t)}{\partial t} = \frac{2\varepsilon}{3m\nu_m(\varepsilon)} \nabla^2 n + \frac{1}{3} \varepsilon_0 \nu_m(\varepsilon) \frac{\partial n}{\partial \varepsilon} + \frac{2}{3} \varepsilon_0 \nu_m(\varepsilon) \frac{\partial^2 n}{\partial \varepsilon^2} + F, \quad (1)$$

where  $n(\varepsilon, t) d\varepsilon$  accounts for the density of electrons at energy between  $\varepsilon$  and  $\varepsilon + d\varepsilon$ ,  $\varepsilon_0 = e^2 E^2 / 2m\omega^2$  refers to the average value of the electron oscillatory energy in the laser field of electric field  $E$  and angular frequency  $\omega$ .  $\nu_m(\varepsilon)$  is the momentum transfer collision frequency and  $e$  and  $m$  are the electronic charge and mass. The first term of this equation signifies the rate of diffusion loss of electrons from the radiated volume. In this analysis, we shall approve the assumption made in Kroll and Watson [9] by writing  $\nabla^2 n = -\Lambda^{-2} n$ , where  $\Lambda$  is the diffusion length. While the second term denotes the amount of energy gained by electrons; the third term describes the diffusion of electrons along the energy axis. This term is obtained from classical arguments based on expressions for the mean energy gain per collision for various types of interactions given by Pert [10] which is analogous to the term involving energy diffusion appeared in the energy gain equation derived by Zel'dovich and Raizer [12] as a consequence of using a quantum-mechanical treatment. The last term,  $F$ , includes the inelastic collisional processes. These processes are responsible for; energy loss by an electron to transfer ground-state atom to any of the considered excited states  $k$ . Also, the production of electrons by ionizing ground-state atoms, as well as a two-step ionization processes via photo and electron impacts ionization of the formed excited atoms.

### 2.2 Krypton data

We apply the model to the case of krypton atom using the following relations for the cross sections and rate coefficients.

#### 2.2.1 Momentum transfer cross section

Because of the Ramsauer minimum observed in the experimental cross section of momentum transfer in the collision of electrons with krypton atoms is given by Rappy and Englander-Golden [11], the applied technique of the least-square fitting is represented by two energy regimes as follows:

$$\begin{aligned} \sigma_m(\epsilon) &= 9.00708 \times 10^{-17} - 3.5076 \times 10^{-16}\epsilon + 5.01069 \times 10^{-16}\epsilon^2 - 2.12642 \times 10^{-16}\epsilon^3 \\ &\quad + 4.69654 \times 10^{-17}\epsilon^4 - 4.06048 \times 10^{-18}\epsilon^5 \quad 0.5 < \epsilon < 4.0 \text{ eV} \\ \sigma_m(\epsilon) &= -5.53067 \times 10^{-15} + 2.49487 \times 10^{-15}\epsilon - 3.843 \times 10^{-16}\epsilon^2 + \\ &\quad 3.10156 \times 10^{-17}\epsilon^3 - 1.38562 \times 10^{-18}\epsilon^4 + 3.2273 \times 10^{-20}\epsilon^5 - 3.04384 \times 10^{-22}\epsilon^6 \quad 4.0 < \epsilon < 30 \text{ eV} \end{aligned} \tag{2}$$

2.2.2 Collisional excitation cross section

The excitation cross section of the two considered excited states is performed using a least-square fitting technique to the experimental data given by Rapp and Englander-Golden [11]. These are written as:

$$A = \frac{\sigma^q}{v^{2q-1}(q-1)!h^q}, \tag{6}$$

where  $\sigma$  is the absorption cross section of atoms and it is taken to be  $\sigma = 10^{-16} \text{ cm}^2$ ,  $v$  is the laser frequency and  $q$  is the number of absorbed photons required to ionize a krypton atom, and  $h$  is Planck's constant.

$$\begin{aligned} \sigma_{\text{ex1}}(\epsilon) &= 2.31039 \times 10^{-16} - 1.05117 \times 10^{-16}\epsilon + 1.54377 \times 10^{-17}\epsilon^2 \\ &\quad - 9.66605 \times 10^{-19}\epsilon^3 + 2.75988 \times 10^{-20}\epsilon^4 - 2.96117 \times 10^{-22}\epsilon^5 \quad \epsilon > 9.91 \text{ eV} \\ \sigma_{\text{ex2}}(\epsilon) &= 1.22992 \times 10^{-15} - 3.16653 \times 10^{-16}\epsilon + 2.93885 \times 10^{-17}\epsilon^2 \\ &\quad - 1.20622 \times 10^{-18}\epsilon^3 + 2.21871 \times 10^{-20}\epsilon^4 - 1.43323 \times 10^{-22}\epsilon^5 \quad \epsilon > 10.03 \text{ eV} \end{aligned} \tag{3}$$

2.2.3 Collisional ionization cross section of ground-state atoms

For ionizing ground-state krypton atom by electron impact the cross section is obtained from least-square fit to the experimental data given by Rapp and Englander-Golden [11] which is written as

The calculated rate coefficient together with the corresponding number of the absorbed photons required to ionize a ground and excited krypton atoms are calculated and shown in the Table 1.

$$\begin{aligned} \sigma_i(\epsilon) &= 3.21216 \times 10^{-15} - 8.02339 \times 10^{-16}\epsilon + 7.56139 \times 10^{-17}\epsilon^2 - 3.40042 \times 10^{-18}\epsilon^3 \\ &\quad + 7.50396 \times 10^{-20}\epsilon^4 - 6.53835 \times 10^{-22}\epsilon^5 \end{aligned} \tag{4}$$

$\epsilon > 14.0 \text{ eV}$

2.2.4 Cross section of stepwise collisional ionization

Owing to the deficiency of the available experimental data for these cross sections, as an approximation the same functional form of ionization of ground-state atoms multiplied by a factor of 100 was considered as follows [2]:

$$\begin{aligned} \sigma_{\text{ieX}}(\epsilon) &= [3.21216 \times 10^{-15} - 8.02339 \times 10^{-16}\epsilon + 7.56139 \times 10^{-17}\epsilon^2 - 3.40042 \times 10^{-18}\epsilon^3 \\ &\quad + 7.50396 \times 10^{-20}\epsilon^4 - 6.53835 \times 10^{-22}\epsilon^5] \times 10^2, \end{aligned} \tag{5}$$

$\epsilon > (14.0 - E_{\text{exk}}) \text{ eV}$

where  $E_{\text{exk}}$  is the excitation energy of an atom in an excited state  $k$  ( $= 1$  and  $2$ ).

2.2.5 Multiphoton ionization rate coefficient

The rate coefficient of multiphoton ionization of ground and excited Kr atoms is calculated using a relation  $A = \frac{\sigma^q}{v^{2q-1}(q-1)!h^q}$  given by Morgan [8] such as:

2.2.6 Electron diffusion rate

During the laser pulse diffusion losses can take place with a high probability of the low gas pressure values. The rate coefficient of free-electron diffusion is given as [9]:

$$v_D = 2\epsilon / (3m\Lambda^2 v_m(\epsilon)), \tag{7}$$

where  $\Lambda$  is the diffusion length of electrons in a cylindrical focal volume and is determined from the relation  $\Lambda = r_0/2.405$ ,  $r_0$  is the radius of the cylindrical focal volume.

The model also takes into account the depletion of ground-state atoms due to ionization and excitation. Step excitation transitions are neglected due to the lack of the data available for their cross sections.

### 2.3 Calculation

Equation [1] is solved numerically applying a step-by-step integration technique. The energy step length  $\Delta\epsilon$  was taken to be such that the whole distribution of the electrons energy could be represented by about 30 equally spaced points since the ionization level of krypton corresponds to the energy of 14.0 eV. The finite difference method is used to evaluate the derivatives  $\partial n/\partial\epsilon$  and  $\partial^2 n/\partial\epsilon^2$ .

Following our original paper [2], to avoid discontinuities in the electron energy distribution function  $n(\epsilon)$ , it is assumed that a low-energy single electron is present in the interaction volume. This electron is represented as a Gaussian distribution of mean energy 4.0 eV and standard deviation 2.0 eV, (the fractional numbers of electrons in each energy range must be given a statistical interpretation, at small times). Moreover, the inelastic collisional excitation and ionization processes (the term,  $F$ , in the basic differential Eq. 1), are treated separately.

A Gaussian shape is assumed to the temporal variation of the laser pulse which is written as

$$I(t) = I(o)a_l \left( e^{-\frac{(t-\tau)^2}{4\tau^2}} - b_l \right), \quad (8)$$

where  $a_l$  and  $b_l$  are constants,  $I(o)$  is the laser peak intensity at time  $\tau$  and  $2\tau$  is the FWHM of the laser pulse.

The focal region  $V$  is estimated using the relation:

$$V = \pi r_0^2 (2\sqrt{2} - 1) (f_l^2 \theta_l) / D_l, \quad (9)$$

where  $r_0$  is the radius of focal region,  $f_l$  is the focal length of the focusing lens,  $\theta_l$  is the beam divergence, and  $D_l$  is the unfocused beam diameter.

In this work, the breakdown criterion is taken as the achievement of a percentage of ionization  $\delta \approx 0.1\%$  of the neutral gas atoms existing in the interaction region.

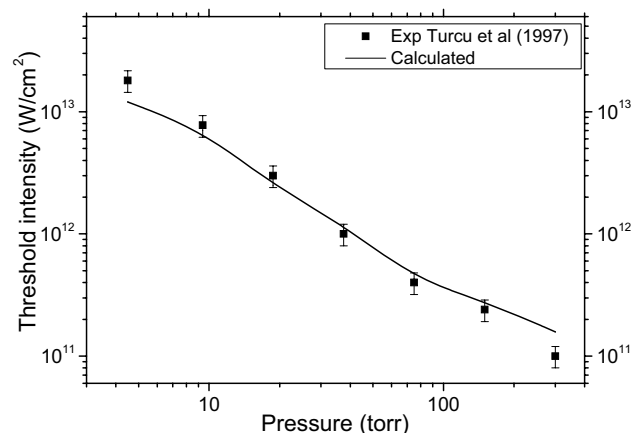
### 3 Results and discussion

Figure 1 shows a comparison between the calculated breakdown threshold intensity as a function of gas pressure (curve 1), and the measured ones (solid squares) corresponding to the experimental conditions given by Turcu et al. [1]. Reasonable agreement is presented; both thresholds showed unexpectedly sharp slope over the experimentally tested pressure range. This agreement validated the model.

To find out the reason for this slope the relationship between the physical processes responsible for breakdown and gas pressure was studied. In doing so, Fig. 2 presents the calculated EEDF at the peak (a) and ended (b) of the laser pulse for selected values of the gas

pressure namely: (1) 4.5 torr, (2) 18.8 torr, (3) 75 torr, and (4) 300 torr. From this figure, it is noticed that for the lower pressure region (graphs 1, and 2) the EEDF calculated at the peak (curve a) lies above those obtained at the end of the pulse (curve b) with their tail extended to electron energy range much above the ionization limits (14.0 eV). This result indicates the low rate of inelastic collisions, while the low values shown by curve (b) confirm the significance of electrons loss by diffusion out of the focal region during the second half of the laser pulse. At the higher pressure regime (graphs 3 and 4), the case is reversed where the values of the EEDF obtained at the peak (curve a) lie below those calculated at the end of the pulse (curve b). This behavior showed the high rate of electron generation through inelastic collisional processes which can easily compensate electrons loss by diffusion. This is indicated by the sharp decrease of the EEDF immediately after the upper excitation threshold ( $>10.0$  eV), with its tail directed towards the low-energy region.

Figure 3 represents the time evolution of the number of electrons in the focal volume calculated for the four pressure values shown by the curves (1–4). It is noticed here that, despite the value of the gas pressure, the time evolution of electrons did not show any immediate growth after firing the laser source, all started with 1.0 electron. The slight decrease of the electrons number throughout the beginning of the laser pulse shown for the low-pressure values (graphs 1 and 2) is attributed to the actual contribution of diffusion losses. While the fast growth of electrons illustrated by these curves up to a time exceeding the pulse peak is referred to the high ionization rate by photoionization of ground and excited state atoms. Beyond the peak, another decrease is observed up to its



**Fig. 1** Comparison between the calculated (*solid line*) and measured (*scattered solid squares*) threshold intensity as a function of gas pressure

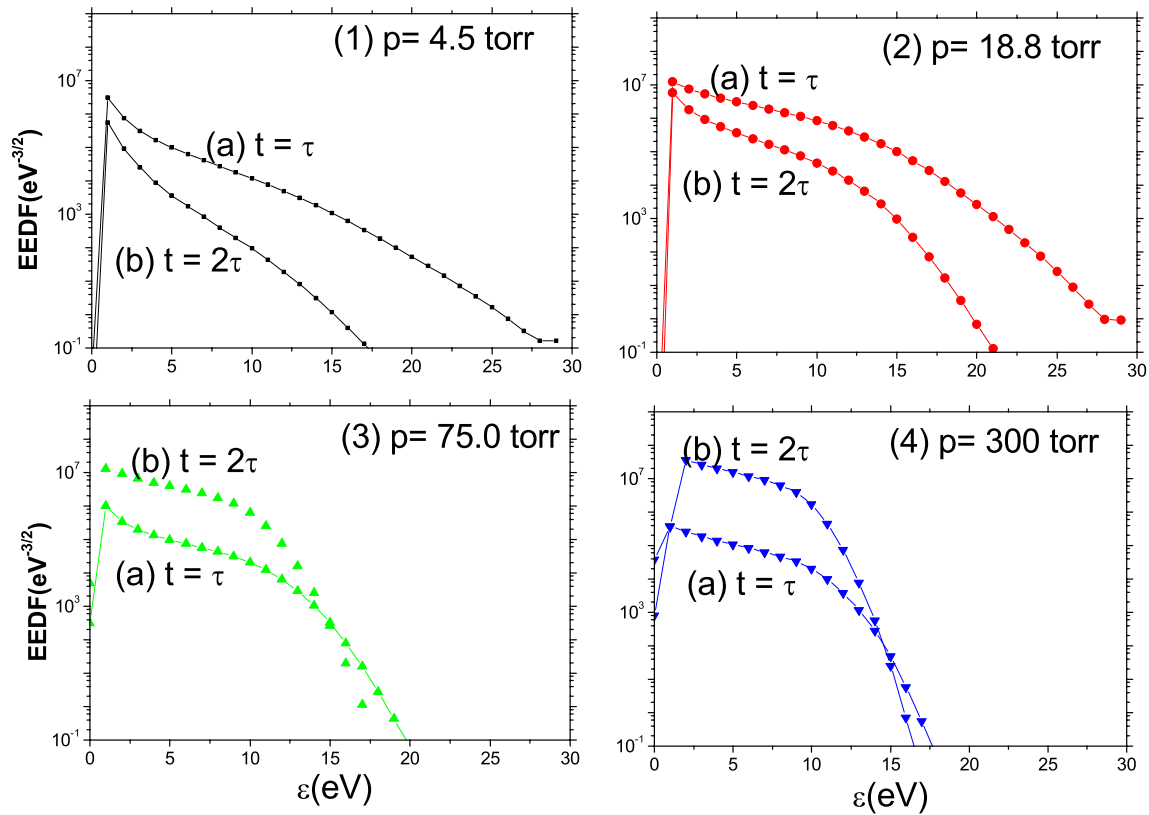


**Fig. 2** EEDF plotted at the peak (curve a) and end (curve b) of the laser pulse for gas pressure: 1 4.5 torr, 2 18.8 torr, 3 75.0 torr, and 4 300 torr

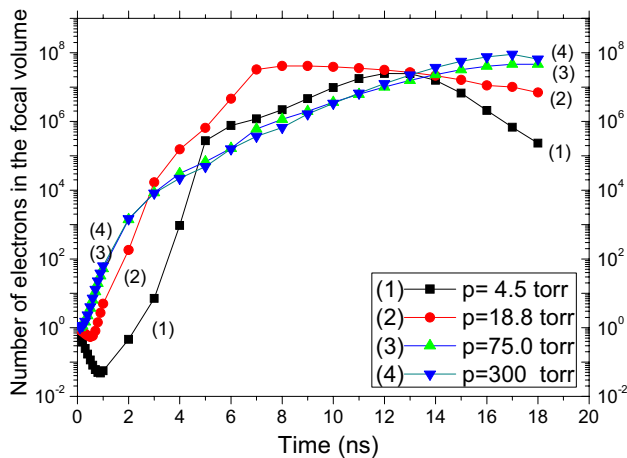


**Fig. 3** Time evolution of the electron density calculated for the four values of the gas pressure

end. This result assured that through the initial period of the pulse (where the laser intensity is low), electron diffusion competes with electron generation by photoionization. This, competition turns to slightly retard the growth of electrons. The decrease of the number of electrons shown during the descending phase of the pulse clarifies the domination of this loss process when the laser

intensity is in its decreasing state. This result confirms the lower values of the EEDF shown by curve (b) in Fig. 2.

At higher pressures (curves 3 and 4), however, the electron growth showed a gradual increase up to the end of the laser pulse. This result proves the lower contribution of electron diffusion during the early stages of the pulse, besides it verified that electron growth is achieved by the combined effect of collisional and photoionization processes of the ground and excited gas atoms which led eventually to a state of breakdown.

The number of ionization per electron per ns is calculated as a function of time for the four selected pressure values and shown in Fig. 4. From this figure, it is noticed that all the curves (1–4) display a peak. The position of such peak is found to correspond to a time interval that depends on the gas pressure. For the lower pressures (curve 1 and 2) the peak appeared at 4.0 ns with a noticeable width that covers almost the first 7.0 ns of the laser pulse. This behavior confirms the fast growth of the electrons number due to photoionization process. While for the high pressures (curves 3 and 4), the peak appeared earlier (at 1.0 ns), then after the number of ionization per electron per ns decreases to a low value (close to zero eV) which is continued up to the end of the pulse. This behavior is consistent with the slow growth of electrons followed by an almost leveling off

state near the end of the pulse by curves (3 and 4) shown in Fig. 3. The peak appeared during the initial stages of the laser pulse could be attributed to the photoionization of the excited atoms. While the low value of the number of ionization per electron per ns is referred to the electron energy losses through collisional excitation processes which are effective during the second half of the pulse. The later process depends on the rate of energy gained by electrons from the laser field. This process is mainly influenced by the rate of the momentum transfer between electrons and krypton gas atoms. For this gas, this rate suffers from Ramsauer minimum [13], leading to this slow growth of the ionization.

Figure 5 represents the temporal change of the calculated mean electron energy at carefully chosen pressures. It is shown from this figure that during the rising part of the laser pulse the mean electron energy showed discriminate behavior for the two tested gas pressure regimes, where for

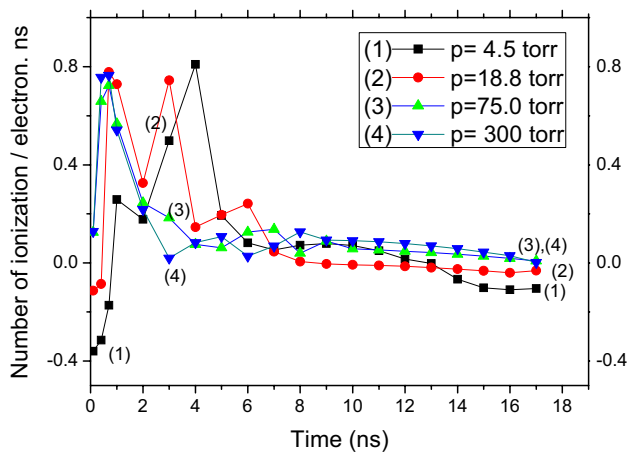
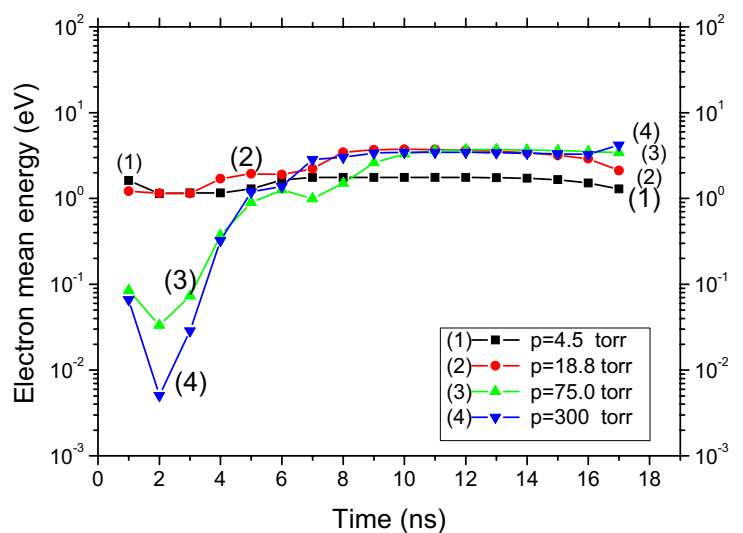


Fig. 4 The number of ionization per electron per ns calculated for the selected pressure values

Fig. 5 Time variation of the electron mean energy obtained at the considered four gas pressures



the low-pressure region curves (1 and 2) it displayed negligible variation over the whole pulse length. This behavior proved that ionization at these pressures proceeds via photoionization of ground and excited Kr atoms. This process leads to the formation of high density of low-energy electrons which can absorb energy through the inverse Bremsstrahlung absorption process.

This energy is then used in collisional excitation. Thereafter the mean electron energy attained a constant value (~1.6 eV) up to the end of the pulse. This saturation behavior specifies the competition between electron generation by photo-ionizing the populated excited states and losses by electron diffusion out of the focal volume. On the other hand, for the high-pressure regime (curves 3 and 4) a noticeable decrease is observed during the early stages of the pulse exhibiting a minimum of  $3 \times 10^{-3}$  eV at 2.0 ns. This decrease reflected the high loss rate of the electrons energy through inelastic collision processes. Following this minimum, these curves showed fast increase reaching a value of 3.5 eV, which is continued over the remaining time of the pulse. This result, however, indicates the low rate of energy gain by electrons and hence the less effect of inelastic collisions throughout the second half of the laser pulse. Moreover, the constant value shown on the second half of the pulse for all pressures is consistent with the behavior of the temporal growth rate of the electrons number shown in Fig. 3.

Figure 6 illustrates the EEDF calculated at different time intervals during the laser pulse for gas pressure values ranging from 4.5 torr to 300 torr (top). The bottom part of this figure shows contour representation of this relation. This diagram determines the time at which breakdown occurs, the energy region corresponding to the generated electrons as well as the distribution of the electrons density in the surrounding ionized zones. It seems from this figure

that, despite the value of the gas pressure is, the temporal variation of the EEDF does not follow a Maxwellian distribution, but rather it showed different rates of growth on the rising and descending parts of the laser pulse.

On the other hand, it is noticed that at a pressure 4.5 torr (Fig. 6a) the calculated EEDF starts with low values then it increases slowly during the first 2 ns, followed by a rapid

increase on the interval 4 ns to 8 ns where a maximum value is reached at 12 ns (ie after the peak of the pulse). Beyond this time a gradual decrease followed by a rapid drop is shown on energy range >5 eV. This behavior indicates that ionization takes place in two steps: first through collisional process that gives rise to excitation of atoms, second it followed by their fast photoionization. This result

**Fig. 6** Time evolution of the EEDF during the laser pulse calculated at the chosen values of the gas pressure (*top graph*). Contour representation of this relation is shown in the *bottom diagram*

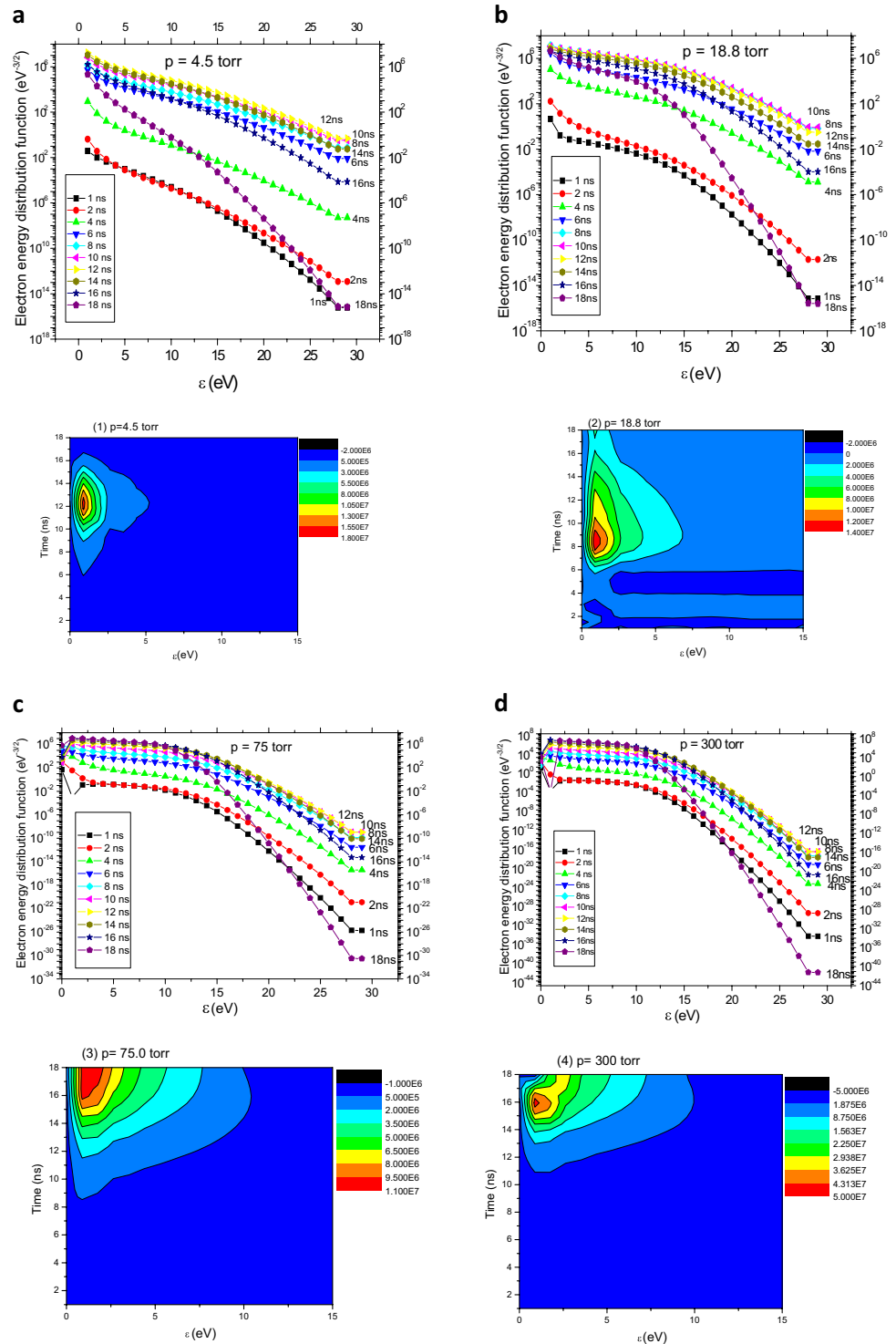


**Table 1** The multiphoton ionization rate coefficient calculated for the excited and ground-state Kr atoms with the corresponding minimum number of photons absorbed by an atom to reach the ionization threshold and the residual energy carried by the emitted electron

Wavelength, nm	Energy of photons absorbed, eV	Ionization energy ( $E_i$ ), eV	Threshold excitation energy ( $E_x$ ), eV	$dE = (E_i - E_{ex})$ , eV	Number of photons absorbed ( $q$ )	Residual energy	Photoionization coefficient ( $\text{cm}^2 \text{w}^{-1}$ ) <sup>q</sup> $\text{sec}^{-1}$
248	4.998	14	9.91	4.09	1	0.908	$1.2473 \times 10^{-2}$
			10.03	3.97	1	1.028	$1.2473 \times 10^{-2}$
			14	14	3	0.994	$6.6265 \times 10^{-37}$

is clarified by the contour representation diagram shown in the bottom of Fig. (6a) in which the breakdown is represented by the red region surrounded by ionization zones of degradation colors. This figure clarified that breakdown occurs throughout the second half of the laser pulse immediately after the pulse peak at a span of time that falls between 12 and 13 ns, with electrons of energy  $\sim 1.0$  eV. Moreover, ionization zones of decaying electron density surrounding the breakdown area are also shown.

At the pressure of 18.8 torr, the EEDF is slowly increasing during the early stages of the laser pulse followed by a rapid increase as it gets closer to the pulse peak (top part of Fig. 6b). Thereafter, a gradual decrease of the EEDF is observed followed by a state of leveling of behavior during the period 8–14 ns. Beyond this time fast decrease is shown resulting in a tail directed towards the low-energy region. This decrease explains the high electron energy loss through inelastic collisional processes leading to excitation and ionization of the gas atoms. This behavior of the EEDF is demonstrated clearly in the contour representation diagram shown in the bottom part of Fig. 6b. This diagram determined that at this pressure breakdown is formed near the peak of the pulse with electrons corresponding to 0.0 eV, and surrounded by ionization zones (with decaying electron densities as shown by the colored band) extended over the last half of the laser pulse with a broader energy range.

This study also indicated that increasing the gas pressure to a value of 75.0 torr (Fig. 6c) results in different temporal behavior of the EEDF. This is observed from the relatively constant growth rate of the EEDF over the low electron energy region during the first half of the laser pulse. On the other hand, during the latter half of the pulse a noticeable increase of the EEDF is observed followed by fast decay with its tail in the low-energy region. Thus this study revealed that at this gas pressure value breakdown is formed at the end of the pulse which proves that ionization is mainly governed by cascade ionization process where the electrons lose their energy in exciting and ionizing the gas atoms leading ultimately to breakdown and plasma generation. The contour diagram shown in the bottom part of this figure confirms this result where it shows the breakdown area confined at the end of the laser pulse with electrons

carrying energy up to 2.0 eV (represented by the red color area) surrounded by ionization zones that are widespread at higher electron energy.

At the higher gas pressure 300 torr, Fig. (6d) showed similar temporal variation behavior of the EEDF as that shown in Fig. 6c. Accordingly the breakdown is perceived at time around 16 ns and is confined to a very small area corresponding to electron energy of  $\sim 1.0$  eV (red color shown in the bottom part of Fig. 6d). Above this time the EEDF suffered from an apparent decrease up to the end of the pulse. This decrease in turn, results in a reduction of the electron density below the breakdown criteria leading to the formation of the ionization regions that are extended to a wide energy region surrounding the breakdown area. This again is attributed to the fact that near the peak of the pulse electrons lose their energy through inelastic collisional processes that lead to a rapid atomic excitation followed by photo and collisional ionization at low rate due to the decrease of the laser intensity during its decline phase.

## 4 Conclusion

In this work, a previously developed numerical electron cascade model [2] is modified and applied to investigate the origin of the steep slope observed in the measurements of the threshold intensity against gas pressure for krypton irradiated by 248 nm laser radiation with pulse duration of 18 ns [1]. The computations revealed a good agreement between the calculated thresholds and the experimentally measured ones. This agreement validates the model. The exact contribution of each physical process to the breakdown mechanism is examined by studying the EEDF and its parameters over the selected values of the experimentally tested gas pressure range (4.5–300 torr). This study revealed that electron diffusion out of the focal volume dominates over pressures  $< 75$  torr. On this pressure regime, it is well known that (see for example, Morgan [8]) photoionization process of ground and excited state atoms are expected to be the main source of free electrons. So pressure independence of the threshold intensity should be predicted. Consequently, the obtained result gives evidence that electron diffusion is responsible for the steep slope



shown in the relation between the threshold intensity and gas pressure observed experimentally.

Moreover, this investigation clarified that over the experimentally studied pressure range inelastic collisions act mostly to convert ground-state atoms into the excited states where photo and collisional ionization of these states take place. The latter process is found to be more effective on pressures  $>75.0$  torr. Analyzing the contour illustration of the time evolution of the EEDF enabled the determination of the dependence of plasma ignition time during the laser pulse, the electrons energy region as well as the extension of the surrounded ionization zones on the gas pressure in laser induced krypton breakdown.

## References

1. I.C.E. Turcu, M.C. Gower, P.H. Huntington, (1997) *Optics Commun.* 13 4, 66–68.
2. C. Evans, Y.E.E.D Gamal, *J Phys D Appl. Phys.* **13**, 1447–1458 (1980)
3. Y.E.E.D Gamal, L. El-Nadi, M.O. Oma, B. Ghazoulin, K.A. Sabour, *J. Phys. D Appl. Phys.* 32, 1633–1639 (1999). (Printed in the UK)
4. Y.E.E.D. Gamal, M.S. Shafik, *J. Phys. D Appl. Phys.* 26, 767–772 (1993) (Printed in the UK)
5. Y.E.E.D. Gamal, M.A.E.H. Mahmoud, N.D.A. Dawood, *Eur. Phys. J. D* 68: 206 (2014).doi:[10.1140/epjd/e2014-50111-x](https://doi.org/10.1140/epjd/e2014-50111-x)
6. Y.E.E.D. Gamal, G. Abdellatif, *Appl. Phys. B*. doi:[10.1007/s00340-014-5807-0](https://doi.org/10.1007/s00340-014-5807-0), Springer, Berlin, Heidelberg 2014. Published on line: 01 April 2014
7. Y.E.E.D. Gamal, I.M. Azzouz, *J. Phys. D Appl. Phys.* 34,1 (2001)
8. C.G. Morgan, *Rep. Prog. Phys.* 38, 621–665 (1975)
9. N. Kroll, K.M. Watson, *Phys. Rev. A* **5**(4), 1883–1905 (1972)
10. G.J. Pert, *J. Phys. A Gen. Phys* **5**, 506 (1972)
11. D. Rappy, P. Englander-Golden, *J. Chem. Phys.* 43, 1464–1479 (1965)
12. Y.B. Zel'dovich, Y.P. Raizer, *Sov. Phys. JETP* **20**, 772–780 (1965)
13. M. Hayashi, Report of At. Data, IPP/Univ. of Nogoya, (1981)